Submitted to Nuclear Physics

RECEIVED
LAWRENCE
RADIATION LABORATORY

FEB 8 1974

LIBRARY AND
DOCUMENTS SECTION

LBL-2321
Preprint

INFLUENCE OF PAIRING AND OF THE SPIN PROJECTION DISTRIBUTION ON THE "CLASSICAL" ISOTHERMAL ROTATIONS OF A NUCLEUS

L. G. Moretto

January 1974

Prepared for the U. S. Atomic Energy Commission
under Contract W-7405-ENG-48

TWO-WEEK LOAN COPY

This is a Library Circulating Copy which may be borrowed for two weeks. For a personal retention copy, call Tech. Info. Division, Ext. 5545

LAWRENCE BERKELEY LABORATORY
UNIVERSITY OF CALIFORNIA
BERKELEY

LBL-2321

DISCLAIMER

This document was prepared as an account of work sponsored by the United States Government. While this document is believed to contain correct information, neither the United States Government nor any agency thereof, nor the Regents of the University of California, nor any of their employees, makes any warranty, express or implied, or assumes any legal responsibility for the accuracy, completeness, or usefulness of any information, apparatus, product, or process disclosed, or represents that its use would not infringe privately owned rights. Reference herein to any specific commercial product, process, or service by its trade name, trademark, manufacturer, or otherwise, does not necessarily constitute or imply its endorsement, recommendation, or favoring by the United States Government or any agency thereof, or the Regents of the University of California. The views and opinions of authors expressed herein do not necessarily state or reflect those of the United States Government or any agency thereof or the Regents of the University of California.

INFLUENCE OF PAIRING AND OF THE SPIN PROJECTION DISTRIBUTION ON THE "CLASSICAL" ISOTHERMAL ROTATIONS OF A NUCLEUS*

L. G. Moretto

Department of Chemistry and
Lawrence Berkeley Laboratory
University of California
Berkeley, California 94720

January 1974

Abstract

The properties of spherical, paired nuclei with finite angular momentum are discussed in terms of "classical" rotations. Rotational quantities like the angular velocity and the moment of inertia are calculated both for the yrast line (T = 0) and for higher temperatures. Particular attention is paid to the superfluid features associated with the pairing correlation. Three different models are considered. The first model is characterized by a constant spacing in the single particle levels and by a constant spin projection, and it is treated analytically in the zero temperature limit. It is shown that this model leads to a very strong back-bending. Calculations accounting for the pairing fluctuations are shown. The second model differs from the first one in the spin projection distribution which, in analogy with a spherical shell model nucleus, is taken to be rectangular. Analytical calculations show that, while strong superfluid properties remain, the back-bending seen in the previous model disappears. The third model used is the shell model. Numerical calculations of the angular velocities and of the moments of inertia are compared with the results obtained from the previous two models. A remarkable agreement is observed between the second model and the shell model.

*Work performed under the auspices of the U. S. Atomic Energy Commission.

I. Introduction

It has been shown that the main effect of angular momentum on the nuclear level density can be accounted for, on one hand by the rotational phase space of the nucleus as a whole, on the other by the unavailability of the rotational energy to excite the intrinsic degrees of freedom[1a,1b]). This rotation and the associated rotational phase space need not be associated with well defined rotational quantum states. In fact, such a rotation is present even in the case of a spherical nucleus where no quantum mechanical rotation is possible.[1a] These rotational features are essentially "classical" in nature insofar as the rotational strength is shared by all the states. Along the same line, individual levels may not show any distinct rotational characteristics, while the envelope of many levels shows an energy-angular momentum dependence typical of a rotor. This is expected to be the case for the yrast line of a spherical nucleus: the individual yrast levels may not show a rotational behavior individually, since they are not part of a rotational band. However their envelope is expected to show distinct rotational features. A similar consideration should hold also for nuclei at temperatures larger than zero.[†]

[†]The use of temperature as a meaningful nuclear parameter has not received the recognition it may deserve. The usual objection is that a nucleus is a system with fixed energy and not with fixed temperature. This is not quite true if one considers the ensemble of nuclei produced in a compound nucleus decay (e.g. neutron emission) or when an individual degree of freedom in equilibrium with the remaining intrinsic degrees of freedom is singled out (e.g. the fission mode at the nuclear saddle point). In all of these cases the temperature and not the energy is constant. In many cases it is peculiar to see a great effort being made to calculate constant energy properties followed by an equally great effort to fold the same properties over distributions which are characterized quite simply by a constant temperature.

The existence of rotational features in the energy-angular momentum isotherms allows one to extract other rotational quantities like the angular velocity and the moment of inertia.

A model with uniform single particle spacing and uniform spin projection distribution is characterized by a constant moment of inertia whose value corresponds to the "rigid" value[2]). A shell model with nonuniform spacing and spin projection distribution still yields a "rigid" moment of inertia. However such a moment of inertia is not constant insofar as changes in temperature and in angular momentum can lead to the occupation of levels with widely different spin projections. In general the presence of residual interactions still leads to a rigid moment of inertia. Only special residual interactions such as those of the pairing kind produce moments of inertia which deviate dramatically from their rigid value. Such interactions are responsible for a superfluid condensation which leads to a highly correlated motion of the nucleons.

The effect of the pairing interaction on the quantum mechanical rotations namely on the rotational bands of deformed nuclei has been studied theoretically[3]). The antipairing effects of angular momentum are shown to reduce dramatically the correlation, to increase the moment of inertia and to lead to a backbending in the plot of the moment of inertia versus the square of the angular velocity. The experimental evidence of reduced moments of inertia in rotational bands and the observation of backbending[4-8]) has been interpreted as evidence of the pairing correlation.

In the present paper we are interested in determining the effect of the pairing residual interaction on the "classical" rotations of a spherical

nucleus at various temperatures and angular momenta. In particular sec. 1 is devoted to the presentation of the formalism. In sec. 2 the formalism is applied to a model with constant spacing and constant single particle spin projection. The expressions for the yrast energies and for the T = 0 limit of the angular velocity and moment of inertia are derived. The extension of the calculation to finite temperatures indicates the presence of a backbending in the moment of inertia-angular velocity plot which disappears as the temperature increases. In sec. 3 the pairing fluctuations are studied and the collective rotational quantities are recalculated with a new formalism accounting for the fluctuations. The sharp boundary between superfluid and normal phase is shown to disappear.

In sec. 4 the relevance of the spin-projection distribution on the detailed dependence of the yrast energy and of the angular velocity upon the angular momentum is studied. It is shown that a rectangular spin projection distribution, which is a more realistic description of the actual spin projection distributions, implies the disappearance of the backbending even at zero temperature.

In sec. 5 the Nilsson model is used to obtain a more realistic description of spherical nuclei and the results are compared with those obtained from the analytical models.

2. General Formalism

The pairing Hamiltonian used in this paper is characterized by a constant pairing strength G:

$$H = \sum \varepsilon_k \, a_k^\dagger \, a_k - G \sum a_{k'}^\dagger \, a_{\bar{k}'}^\dagger \, a_{\bar{k}} \, a_k \quad , \tag{1}$$

where ε_k are the single particle energies and $a_k^\dagger$ and a_k are the creation and destruction operators respectively. The Hamiltonian can be rewritten in the quasiparticle space as follows:

$$H' = 2 \sum v_k^2 (\varepsilon_k - \lambda) - G \left[\sum u_k v_k (1 - 2\, n_k) \right]^2 + 2 \sum n_k (\varepsilon_k - \lambda)(u_k^2 - v_k^2) \quad , \tag{2}$$

where v_k and u_k are the amplitudes of the particles and holes respectively, n_k are the occupation numbers in the quasiparticle space and λ is the chemical potential. The amplitudes u_k and v_k obey the relation:

$$u_k^2 + v_k^2 = 1 \quad . \tag{3}$$

The requirement that the Hamiltonian be stationary with respect to v_k with n_k kept constant leads to the gap equation:

$$\sum \frac{1 - 2\, n_k}{E_k} = \frac{2}{G} \quad , \tag{4}$$

where $E_k = [(\varepsilon_k - \lambda)^2 + \Delta^2]^{1/2}$ and where n_k are the occupation numbers of quasiparticles. The following expressions for v_k^2 and u_k^2 are also obtained:

$$v_k^2 = \frac{1}{2}\left(1 - \frac{\varepsilon_k - \lambda}{E_k}\right) \qquad u_k^2 = \frac{1}{2}\left(1 + \frac{\varepsilon_k - \lambda}{E_k}\right) \quad . \tag{5}$$

The introduction of the angular momentum projection M into the Hamiltonian[9] can be handled in the same way as the particle number as follows[10-12]):

$$H = H - \lambda N - \gamma M = \sum (\varepsilon_k - \lambda - E_k) + \sum n_k^+ (E_k - \gamma m_k) + \sum n_k^- (E_k + \gamma m_k) + \Delta^2/G \; ; \quad (6)$$

n_k^+ and n_k^- are the quasiparticle occupation numbers with positive and negative spin projections and γ is a Lagrange multiplier which assumes the meaning of the collective angular velocity:

$$\gamma = \frac{\partial H}{\partial M} \quad . \quad (7)$$

The statistical functions can be written as follows:

$$\Omega = -\beta \sum (\varepsilon_k - \lambda - E_k) + \sum \ln[1 + \exp - \beta(E_k - \gamma m_k)] + \sum \ln[1 + \exp - \beta(E_k + \gamma m_k)]$$

$$- \beta \, \Delta^2/G \quad (8)$$

$$N = \sum [1 - \frac{\varepsilon_k - \lambda}{2E_k} \{\tanh \tfrac{1}{2} \beta(E_k - \gamma m_k) + \tanh \tfrac{1}{2} \beta(E_k + \gamma m_k)\}] \quad (9)$$

$$M = \sum m_k \left[\frac{1}{1 + \exp \beta(E_k - \gamma m_k)} - \frac{1}{1 + \exp \beta(E_k + \gamma m_k)} \right] \quad (10)$$

$$E = \sum \varepsilon_k \; [1 - \frac{\varepsilon_k - \lambda}{2E_k} \{\tanh \tfrac{1}{2} \beta(E_k - \gamma m_k) + \tanh \tfrac{1}{2} \beta(E_k + \gamma m_k)\}] - \Delta^2/G \quad . \quad (11)$$

The quantity Δ is related to β λ, γ by the gap equation:

$$\sum \frac{1}{2E_k} [\tanh \tfrac{1}{2} \beta(E_k - \gamma m_k) + \tanh \tfrac{1}{2} \beta(E_k + \gamma m_k)] = \frac{2}{G} \quad . \quad (12)$$

At fixed temperature T or β eqs. (9), (10), and (12) can be solved for Δ, γ λ if N and $M \equiv I$ are given.† The moment of inertia can then be obtained by the relation:

$$\mathfrak{J}\gamma = I \quad . \tag{13}$$

In general the moment of inertia depends upon angular momentum through the dependence of the gap parameter Δ upon the angular velocity. Such a dependence is very strong and produces dramatic changes in the moment of inertia. This has important consequences in the evaluation of the angular momentum dependence of the nuclear level density. Some very approximate estimates of such a quantity make use of the spin cut off parameter σ^2 which is taken to be equal to the following expression[13]):

$$\sigma^2 = \frac{1}{2} \sum m_k^2 \operatorname{sech}^2 \frac{1}{2} \beta E_k = \frac{\mathfrak{J}}{\hbar^2 \beta} \quad . \tag{14}$$

This expression can be easily justified by observing that it corresponds to the following limit:

$$\sigma^2 = \lim_{\gamma = 0} \frac{\partial M}{\partial \beta \gamma} \quad . \tag{15}$$

In other words such an approximation implies that the gap parameter Δ does not depend on angular momentum and that the chemical potential λ does not depend on angular momentum. The validity of such an approximation is in fact rather limited as will be seen in the following sections.

---

†For a spherically symmetric system, it is possible to account completely for the total angular momentum I by means of its z projection M [11,12]).

3. The Uniform Model

The effects of the pairing correlation on the rotational properties of nuclei are best observed when the interference of the shell structure is eliminated[10,11,14]. This can be achieved by the use of the uniform model. In this special version of the uniform model the level scheme consists of a set of equidistant, doubly degenerate levels with a density g and with a constant spin projection m. The information concerning the strength of the pairing interaction is contained in the ground state gap parameter Δ_0. An important advantage of this model is the fact that the chemical potential is a constant because of the symmetries inherent to the single particle scheme. For this reason the particle equation can be disregarded and the chemical potential can be set equal to zero. The equations which remain to be studied are the gap equation, the angular momentum equation and the energy equation. For the uniform model they take the following form:

$$\frac{2}{G} = 2g \int_0^S \frac{1}{2E} \{\tanh \tfrac{1}{2}\beta(E - \gamma m) + \tanh \tfrac{1}{2}\beta(E + \gamma m)\}\, d\varepsilon = f(\Delta,\gamma) \tag{16}$$

$$I = 2gm \int_0^\infty \left\{ \frac{1}{1 + \exp \beta(E - \gamma m)} - \frac{1}{1 + \exp \beta(E + \gamma m)} \right\} d\varepsilon \tag{17}$$

$$E = g \int_{-S}^{+S} d\varepsilon\, \varepsilon[1 - \frac{\varepsilon}{2E} \{\tanh \tfrac{1}{2}\beta(E - \gamma m) + \tanh \tfrac{1}{2}\beta(E - \gamma m)\}] - \frac{\Delta^2}{G} \quad . \tag{18}$$

In these equations $S \gg \Delta_0$ is the energy interval above and below the Fermi surface, over which the pairing correlations is active[15].

This set of equations can be integrated analytically at zero temperature ($\beta = \infty$)[14]. Let us consider the angular momentum equation[17]. For $\beta = \infty$ the second

term of the integrand is zero over the entire integration range, while the first term is unity from $\varepsilon = 0$ to $\varepsilon = [(\gamma m)^2 - \Delta^2]^{1/2}$ and zero thereafter. Thus:

$$I = 2mg[(\gamma m)^2 - \Delta^2]^{1/2} \quad . \tag{19}$$

In order to obtain the relationship between I and γ, the gap parameter Δ must be calculated as a function of γ. This can be achieved by integrating the gap equation in the limit of $\beta = \infty$ in the form:

$$f(\Delta_0, \gamma = 0) = f(\Delta, \gamma)$$

or

$$2g \int_0^S \frac{d\varepsilon}{[\varepsilon^2 + \Delta_0^2]^{1/2}} = 2g \int_a^S \frac{d\varepsilon}{[\varepsilon^2 + \Delta^2]^{1/2}} \quad . \tag{20}$$

The lower limit of the right hand side integral is

$$a = [(\gamma m)^2 - \Delta^2]^{1/2} \quad . \tag{21}$$

This lower limit has a very interesting physical significance. It means that, because of the presence of the angular momentum, the range $\pm S$ in the single particle spectrum is not entirely available to the pairing correlation. In fact all the single particle levels contained in the interval $\pm a$ are effectively removed from the reach of the pairing correlation. These levels are occupied by the unpaired nucleons (quasi-particles) necessary to build up the total angular momentum I. The number of quasi-particles is:

$$n = \frac{I}{m} = 2g[(\gamma m)^2 - \Delta^2]^{1/2} \quad . \tag{22}$$

These "blocked" levels are most precious to the pairing correlation because they are closest to the Fermi surface. Therefore it must be expected that the pairing correlation decrease and eventually vanish as the angular momentum increases.

The integrated form of the gap equation is:

$$\operatorname{arcsinh} \frac{S}{\Delta} - \operatorname{arcsinh} \left(\frac{(\gamma m)^2 - \Delta^2}{\Delta^2}\right) = \operatorname{arcsinh} \frac{S}{\Delta_0} \quad . \tag{23}$$

By means of the summation formula for the function arcsinh and by making use of the assumption $S \gg \Delta_0$ one obtains:

$$\frac{1}{2} \frac{\Delta_0^2 - \Delta^2}{\Delta_0} = [(\gamma m)^2 - \Delta^2]^{1/2} \quad , \tag{24}$$

which is the required relation. Before calculating the relationship between the angular momentum I and the angular velocity γ explicitly, let us determine the dependence of the gap parameter upon the angular momentum. By means of Eq. (19) and Eq. (24) the very simple relation is obtained:

$$\frac{\Delta}{\Delta_0} = \left(1 - \frac{I}{gm\Delta_0}\right)^{1/2} = \left(1 - \frac{I}{I_{cr}}\right)^{1/2} \quad , \tag{25}$$

where

$$I_{cr} = gm\Delta_0 \quad . \tag{26}$$

It can be seen that the gap parameter Δ decreases with angular momentum and eventually vanishes at the critical value of the angular momentum I_{cr}.

By using the expressions just developed, the angular velocity and the moment of inertia can finally be calculated:

$$\gamma = \frac{I_{cr}}{\mathcal{J}_R}\left(2 - \frac{I}{I_{cr}}\right) \text{ for } I < I_{cr} \; ; \quad \gamma = \frac{I}{\mathcal{J}_R} \text{ for } I \geqslant I_{cr} \tag{27}$$

$$\mathcal{J} = \frac{I}{\gamma} = \mathcal{J}_R \frac{I/I_{cr}}{2 - \frac{I}{I_{cr}}} \; ; \quad \mathcal{J} = \mathcal{J}_R \text{ for } I \geqslant I_{cr} \; , \tag{28}$$

or

$$\mathcal{J} = \mathcal{J}_R \frac{\Delta_o^2 - \Delta^2}{\Delta_o^2 + \Delta^2} \tag{28'}$$

where $\mathcal{J}_R$ is the rigid moment of inertia, given by:

$$\mathcal{J}_R = 2m^2 g \quad . \tag{29}$$

In Eq. (28) the effect of the pairing superfluidity on the moment of inertia is clearly seen as well as the antipairing effect of the angular momentum (fig. 2a). In fact the moment of inertia goes from zero to its rigid value as the angular momentum increases to zero to the critical value.

Even more striking is the behavior of the angular velocity (eq. (27)). At zero angular momentum the angular velocity takes the value $2\frac{I_{cr}}{\mathcal{J}_R}$ and it <u>decreases</u> to the value $\frac{I_{cr}}{\mathcal{J}_R}$ as the angular momentum increases to its critical value (fig. 1a). We are dealing with a peculiar object which, the smaller the angular momentum, the faster it spins!

The energy equation can also be integrated analytically at zero temperature. Setting $\beta = \infty$ the integral can be written as:

$$E = g\int_{-S}^{+S} \varepsilon d\varepsilon - g\int_{-S}^{-I/2mg} \frac{\varepsilon^2}{E} d\varepsilon - g\int_{I/2mg}^{+S} \frac{\varepsilon^2}{E} d\varepsilon - \frac{\Delta^2}{G} \quad . \tag{30}$$

After a little algebra one obtains:

$$E = -gS^2 - \frac{1}{2} g \Delta^2 + \frac{I}{2m} \left(\frac{I^2}{4m^2 g^2} + \Delta^2 \right)^{1/2} . \tag{31}$$

By subtracting the ground state energy $E_0 = -gS^2 - \frac{1}{2} g \Delta_0^2$ one obtains the equation for the so called yrast line:

$$E_y = \frac{1}{2} g(\Delta_0^2 - \Delta^2) + \frac{I}{2m} \left(\frac{I^2}{4m^2 g^2} + \Delta^2 \right)^{1/2} , \tag{32}$$

which can be rewritten in a more elegant form as:

$$E_y = \begin{cases} \dfrac{I_{cr}^2}{\mathfrak{J}_R} \dfrac{I}{I_{cr}} \left(2 - \dfrac{I}{2I_{cr}} \right) & \text{for } I \leqslant I_{cr} \quad (33) \\[2ex] \dfrac{I_{cr}^2}{\mathfrak{J}_R} + \dfrac{I^2}{2\mathfrak{J}_R} & \text{for } I \geqslant I_{cr} . \quad (34) \end{cases}$$

Such an equation represents the locus of the levels of largest angular momentum at fixed energy, or conversely the locus of the levels of lowest energy at fixed angular momentum. The parabolic dependence of energy on angular momentum typical of a rigid body can be observed for angular momenta larger than the critical value. The yrast energy in eq. (33) is made up of two components: a rotational component plus a term representing the energy increase due to the disappearance of the pairing correlation. We can consider the moment of inertia of the rotating system to be a function of an internal parameter (the gap parameter) which in turn depends upon angular momentum through the condition of minimum total energy. Systems of this kind are quite common. For instance a deformable sphere when set in rotation assumes a spheroidal shape whose eccentricity depends upon the angular momentum through the condition of minimum energy. In

these cases the angular velocity of the system can be easily calculated. By definition the rotational frequency γ is given by

$$\gamma = \frac{\partial H}{\partial I} \quad . \tag{35}$$

However, by taking the total derivative of energy with respect to angular momentum one obtains:

$$\frac{dH}{dI} = \left.\frac{\partial H}{\partial I}\right|_{\Delta} + \left.\frac{\partial H}{\partial \Delta}\right|_{G} \frac{d\Delta}{dI} \quad . \tag{36}$$

It is easily seen that the partial derivative $\frac{\partial H}{\partial \Delta}$, when set equal to zero, is equivalent to the gap equation (at zero temperature) which defines the very value of the gap parameter. It follows that:

$$\gamma = \frac{\partial H}{\partial I} = \frac{dH}{dI} = \frac{dE_y}{dI} \quad . \tag{37}$$

This can be verified immediately by differentiating Eq. (33) and comparing the result with Eq. (27). At this point we are in the position to calculate the loss in pairing correlation energy E^* due to the angular momentum:

$$E^* = E_y - \frac{I^2}{2\mathfrak{J}} = \frac{I_{cr}^{\ 2}}{\mathfrak{J}_R} \frac{I}{I_{cr}} \quad . \tag{38}$$

This quantity is zero for $I = 0$ because the system retains the full condensation energy $C = \frac{1}{2} g\Delta_0^2$ when no angular momentum is present, and it is equal to $\frac{I_{cr}^{\ 2}}{\mathfrak{J}_R} = \frac{1}{2} g\Delta_0^2$ at the critical angular momentum when all of the condensation energy due to the pairing correlation is lost. It is also not so surprising to observe that, since the yrast energy at the critical angular momentum is:

$$E_{y_{I = I_{cr}}} = \frac{3}{2} C \quad , \tag{39}$$

it follows that the energy in the form of rotational kinetic energy is one half of the energy in form of pairing potential energy. This is just a specific case of the virial theorem.

Let us now consider the more general case in which the temperature is different from zero. It is well known that at zero angular momentum the theory predicts a critical temperature:

$$T_{cr} = \frac{2\Delta_0}{3.5} \quad , \tag{40}$$

at which the pairing correlation disappears.

Before proceeding any further, it is interesting to point out that the system is completely characterized by three critical quantities, the critical temperature, the critical angular momentum and the rigid moment of inertia. These three quantities can be obtained by a suitable combination of the initial parameters of the model g, m, Δ_0

$$T_{cr} = \frac{2\Delta_0}{3.5}$$

$$I_{cr} = mg\Delta_0$$

$$\mathcal{J}_R = 2gm^2 \quad . \tag{41}$$

In this way it is possible to express all the properties of any system by means of three fundamental reduced variables T/T_{cr}, I/I_{cr}, $\mathcal{J}/\mathcal{J}_R$.

As the temperature increases, new quasi particles are created and the gap parameter eventually vanishes. A rather peculiar effect

in the dependence of the gap parameter on temperature at constant angular momentum can be observed. An initial increase in temperature leads to an increase in the gap parameter which is the more substantial the larger the angular momentum. This effect, called thermally assisted pairing correlation[10,11]), is particularly visible in the dependence of the critical angular momentum upon temperature at low temperatures, where an increase in temperature leads to an increase of the critical angular momentum.

Returning to the discussion of the rotational properties, the angular velocity can be obtained by solving the gap equation and the angular momentum equation simultaneously in γ and Δ for a given temperature. A plot of the angular velocity versus angular momentum for various temperatures is shown in Fig. 1a. The zero temperature limit predicted by eq. (27) shows the angular velocity decreasing linearly with angular momentum until the critical angular momentum is reached. Then the angular velocity increases proportionally to the angular momentum. In the lower temperature range, the angular velocity increases very rapidly, reaches a maximum and then decreases until the critical angular momentum associated with the specific value of the temperature is reached. In the upper temperature range, the angular velocity increases monotonically with angular momentum, initially faster, later slower than the normal behavior until the corresponding critical angular momentum is reached. Above the critical angular momenta, the angular velocity is independent of temperature and it increases proportionally to the angular momentum. The dependence of the moment of inertia on angular momentum for various temperatures is shown in Fig. 2a. The zero temperature dependence is given by eq. (28). The moment of inertia is seen to increase regularly with angular momentum until it reaches

the rigid value at the critical angular momentum. However a more peculiar picture is seen when the moment of inertia is plotted as a function of the square of the angular velocity as now fashionable (fig. 3a). A back bending is observed in all those isotherms for which a decrease in angular velocity is observed as a function of angular momentum. The back bending disappears at the higher temperatures. The existence of the back bending in the moments of inertia associated with the ground state rotational band of deformed nuclei has been predicted in various calculations. There seem to be experimental evidence of such a feature in some deformed rare earth nuclei. The present calculation, indicates that analogous features might be present along the yrast line and higher isotherms of spherical nuclei.

4. Effect of Pairing Fluctuations on Angular Velocity Near the BCS Phase Transition

The formalism illustrated in the previous section predicts that the nuclear superfluidity should disappear abruptly as the gap parameter goes to zero. A phase boundary $f(T, I) = 0$ can be determined in the temperature-angular momentum plane which separates the superfluid from the normal region. The prediction of such a phase transition is correct in the limit of a large number of particles. For a nucleus, where the particle number is small, large fluctuations are to be expected which do remove the sharp phase transition[16]. In order to appreciate the extent to which the system can fluctuate in its superfluid behavior, let us consider the Hamiltonian:

$$H = 2 \sum v_k^2(\varepsilon_k - \lambda) - G\left[\sum_k u_k v_k (1 - 2n_k)\right]^2 + 2\sum n_k(\varepsilon_k - \lambda)(u_k^2 - v_k^2) \quad , \tag{42}$$

where n_k are the quasiparticle occupation numbers and, for simplicity, we disregard the quasiparticle spin projection.

The BCS treatment consists in finding out the value of Δ which minimizes the Hamiltonian at fixed occupation numbers n_k. In fact it is easy to verify that the condition $\frac{\partial H}{\partial \Delta} = 0$ corresponds to the gap equation (4). In order to estimate the extent of the fluctuations one must calculate the second derivative at the equilibrium value of the gap parameter Δ_{eq}:

$$\left.\frac{\partial^2 H}{\partial \Delta^2}\right|_{\Delta=\Delta_{eq}} = \Delta_{eq}^2 \sum \frac{1 - 2n_k}{E_k^3} \left(1 - \frac{G\,\Delta_{eq}^2}{2} \sum \frac{1 - 2n_k}{E_k^3}\right) \quad . \tag{43}$$

In the absence of quasiparticles and for the uniform model one obtains:

the rigid value at the critical angular momentum. However a more peculiar picture is seen when the moment of inertia is plotted as a function of the square of the angular velocity as now fashionable (fig. 3a). A back bending is observed in all those isotherms for which a decrease in angular velocity is observed as a function of angular momentum. The back bending disappears at the higher temperatures. The existence of the back bending in the moments of inertia associated with the ground state rotational band of deformed nuclei has been predicted in various calculations. There seem to be experimental evidence of such a feature in some deformed rare earth nuclei. The present calculation, indicates that analogous features might be present along the yrast line and higher isotherms of spherical nuclei.

4. Effect of Pairing Fluctuations on Angular Velocity Near the BCS Phase Transition

The formalism illustrated in the previous section predicts that the nuclear superfluidity should disappear abruptly as the gap parameter goes to zero. A phase boundary $f(T, I) = 0$ can be determined in the temperature-angular momentum plane which separates the superfluid from the normal region. The prediction of such a phase transition is correct in the limit of a large number of particles. For a nucleus, where the particle number is small, large fluctuations are to be expected which do remove the sharp phase transition[16]). In order to appreciate the extent to which the system can fluctuate in its superfluid behavior, let us consider the Hamiltonian:

$$H = 2\sum v_k^2(\varepsilon_k - \lambda) - G\left[\sum_k u_k v_k(1 - 2n_k)\right]^2 + 2\sum n_k(\varepsilon_k - \lambda)(u_k^2 - v_k^2) \quad , \tag{42}$$

where n_k are the quasiparticle occupation numbers and, for simplicity, we disregard the quasiparticle spin projection.

The BCS treatment consists in finding out the value of Δ which minimizes the Hamiltonian at fixed occupation numbers n_k. In fact it is easy to verify that the condition $\frac{\partial H}{\partial \Delta} = 0$ corresponds to the gap equation (4). In order to estimate the extent of the fluctuations one must calculate the second derivative at the equilibrium value of the gap parameter Δ_{eq}:

$$\left.\frac{\partial^2 H}{\partial \Delta^2}\right|_{\Delta=\Delta_{eq}} = \Delta_{eq}^2 \sum \frac{1 - 2n_k}{E_k^3}\left(1 - \frac{G\,\Delta_{eq}^2}{2}\sum \frac{1 - 2n_k}{E_k^3}\right) \quad . \tag{43}$$

In the absence of quasiparticles and for the uniform model one obtains:

$$\left.\frac{\partial^2 H}{\partial \Delta^2}\right|_{\Delta=\Delta_{eq}} = 2g\,(1 - gG) \simeq 2g \quad . \tag{44}$$

This implies that, for very small temperatures, the fluctuations in Δ have a width:

$$\sigma \simeq \sqrt{\frac{T}{g}} \propto \sqrt{\frac{T}{N}} \quad . \tag{45}$$

In other words the width of the fluctuations is inversely proportional to the square root of the number of particles. Such a proportionality is, of course, retained even for the more general expression of the second derivative given by eq. (43). Consequently, one does expect that a sharp phase transition may occur in a macroscopic superconductor. On the other hand, on the same basis, such a transition should be washed out when the number of particles is small, like in a nucleus. Because of the finite width of the probability distribution in Δ, and because of the presence of higher moments, the use of average quantities is more significant than the use of the corresponding most probable quantities. The probability distribution in Δ is given by:

$$P(\Delta,\gamma) \propto \exp - (\Omega - \mu M) \quad . \tag{46}$$

Thus the average angular velocity $\bar{\gamma}$ and the average gap parameter $\bar{\Delta}$ are given by:

$$\bar{\gamma} = \frac{\int \gamma P(\Delta,\gamma)\, d\Delta d\gamma}{\int P(\Delta,\gamma)\, d\Delta d\gamma} \quad ; \quad \bar{\Delta} = \frac{\int \Delta P(\Delta,\gamma)\, d\Delta d\gamma}{\int P(\Delta,\gamma)\, d\Delta d\gamma} \quad . \tag{47}$$

The value of γ for a fixed value of Δ, β, and I can be obtained from the angular momentum equation (17). The plot of the average angular velocity versus angular

momentum for various temperatures is shown in fig. 1b. Such a figure should be compared with fig. 1a where the most probable values of the angular velocity are plotted. Away from the critical region the two plots are essentially identical; close to the critical region the most probable angular velocity reaches abruptly its rigid value generating a cusp, while the average angular velocity approaches asymptotically its rigid value. This shows how in a real nucleus one should not expect a phase transition in going from the paired to the unpaired configuration. In fig. 2b the average moment of inertia is shown as a function of angular momentum. As compared with fig. 2a, the rigid moment of inertia is attained only asymptotically at all temperatures instead of abruptly. Notice that, even for $T = T_{cr}$ the moment of inertia is still smaller than its rigid value because of the persistence of the pairing correlation. Similarly in fig. 3b the average moment of inertia is plotted versus the square of the average angular velocity. Again by comparing this plot with fig. 3a one notices the disappearance of the cusps associated with the critical temperatures. In their place a smooth fold over is observed which, for the lowest temperatures constitutes the upper part of an S shaped curve. In fig. 3a the highest isotherm $T = T_{cr}$ gives the rigid moment of inertia. In the new calculation pairing extends above the critical temperature: consequently the isotherm corresponding to $T = T_{cr}$ shows a moment of inertia smaller than its rigid value.

5. Effect of the Spin Projection Distribution Upon the Shape of the Yrast Line

The equidistant model with constant spin projection distribution, considered so far, predicts a decreasing angular velocity with angular momentum in the paired region. As a consequence the yrast line presents a negative second derivative and the plot of the moment of inertia versus the square of the angular velocity shows a backbending.

The above effects depend rather dramatically upon the spin projection distribution. The spin projection used in the previous sections $p(\underline{m})\, d\underline{m} = \delta(\underline{m} - m)\, d\underline{m}$ is not very realistic. In this section a more realistic spin distribution is going to be used[17]). Such a distribution is a rectangular distribution:

$$p(\underline{m})\, dm = \begin{cases} g\,\dfrac{d\underline{m}}{m_x} & \text{for } 0 \leqslant \underline{m} \leqslant m_x \\ 0 & \text{for } \underline{m} \geqslant m_x \end{cases} \quad . \tag{48}$$

Such a distribution approximates the $2j + 1$ projections of a j shell quite well and therefore is expected to be relevant for a spherical nucleus. Also for this distribution it is possible to integrate the angular momentum equation and the gap equation analytically. The angular momentum equation becomes:

$$I = \frac{2}{3}\,\frac{g}{\gamma^2 m_x}\,[\gamma^2 m_x^2 - \Delta^2]^{3/2} \quad . \tag{49}$$

For the gap equation one obtains:

$$\frac{1}{2}\frac{\gamma m_x}{\Delta^2\Delta_o}\left\{(\Delta^2 + \Delta_o^2)\left(1 - \frac{\Delta^2}{\gamma^2 m_x^2}\right)^{1/2} - (\Delta_o^2 - \Delta^2)\right\} = \sinh\left\{\left(1 - \frac{\Delta^2}{\gamma^2 m_x^2}\right)^{1/2}\right\} \quad . \tag{50}$$

The two above equations define the functions $\gamma = \gamma(I)$ and $\Delta = \Delta(I)$ which cannot be expressed analytically. However the limiting values of γ at $I = 0$ ($\Delta = \Delta_o$) and $I = I_{cr}$ ($\Delta = 0$) can be obtained

$$\gamma_{I=0} = \frac{\Delta_o}{m_x} \quad ; \quad \gamma_{I=I_{cr}} = \frac{e}{2}\frac{\Delta_o}{m_x} \quad , \tag{51}$$

where e is the basis of natural logarithms. Therefore

$$\gamma_{I=I_{cr}}/\gamma_{I=0} = \frac{e}{2} > 1 \quad . \tag{52}$$

This means that, contrary to the previous model, the angular velocity is in fact increasing when the angular momentum goes from $I = 0$ to $I = I_{cr}$.

The complete function $\gamma = \gamma(I)$ can be observed in fig. 4: it appears to be a monotonically increasing function of I thus excluding the possibility of backbending. The critical angular momentum and the rigid moment of inertia are given by:

$$I_{cr} = \frac{e}{3}\, g\, m_x\, \Delta_o \quad ; \quad \mathfrak{J}_R = \frac{2}{3}\, g\, m_x^2 \quad . \tag{53}$$

The present model predicts a larger critical angular momentum than the previous model when the comparison is made at constant moment of inertia. The ratio R between the two critical angular momenta is:

$$R = e/\sqrt{3} \quad . \tag{54}$$

The yrast line, which is now expected to have a positive second derivative can be calculated numerically:

$$E_y = \int \gamma \, dI \quad . \tag{55}$$

It is easy to calculate the yrast energy at the critical angular momentum:

$$E_{y(I=I_{cr})} = \frac{1}{2} g \Delta_o^2 + \frac{I_{cr}^2}{2\mathcal{J}_R} = \frac{1}{2} g \Delta_o^2 (1 + \frac{e^2}{6}) \simeq 2.23 \, E_{cond} \quad , \tag{56}$$

where $E_{cond} = \frac{1}{2} g \Delta_o^2$ is the condensation energy due to pairing. This is in contrast with the previous model which predicts $E_{y(I=I_{cr})} = 1.5 \, E_{cond}$. The complete yrast line, presented in fig. 5 shows the expected presence of a small positive second derivative. The difference between the present yrast line and that predicted by the previous model (also shown in fig. 5) is the following. The first quasiparticles to be produced occupy the highest portion of the spin projection distribution; the following quasiparticles occupy orbitals with progressively smaller spin projection. Thus, in order to produce a fixed amount of angular momentum it is necessary to produce a progressively large number of quasiparticles with the consequent requirement of a larger amount of energy as compared with the previous model (the previous model requires always the same amount of quasiparticles for a fixed amount of angular momentum). As a consequence the flaring out of the former yrast line is more than compensated and a nearly linear dependence of the energy upon angular momentum is obtained. The slight overcompensation of the flaring out actually changes the sign of the second derivative and makes it positive.

6. Examples of Calculations Based Upon the Shell Model

A semianalytical study of the properties of simple models has been carried out in the previous sections. It is now interesting to investigate in detail the properties of more realistic models. The shell model, applied to a spherical nucleus, in conjunction with the pairing Hamiltonian, lends itself to a sufficiently simple numerical calculation. In order to simplify the display of the various quantities the calculations are limited to individual nuclear components, neutrons or protons. For a fixed temperature, angular momentum and particle number, the gap equation (12) the angular momentum equation (10) and the particle equation (9) can be solved to give the gap parameter Δ, the angular velocity γ and the chemical potential λ. The angular velocity γ is displayed in fig. 6 as a function of angular momentum for various temperatures for the neutron and proton components of ^{220}Rn. The lowest isotherms show very strong fluctuations due to shell effects for angular momenta above the critical value. For angular momenta lower than the critical value the dependence of γ on angular momentum shows a flatter behavior, which, at the lowest isotherm does indeed resemble the dependence predicted by the uniform model with a rectangular spin projection distribution (fig. 4). So the shell model indicates that at the lowest temperatures the angular velocity tends to become almost constant with angular momentum. Furthermore there is no evidence that the angular velocity decreases with angular momentum. This implies that no backbending is to be expected. The same fig. 6 indicates that as the temperature increases, both pairing and shell effects disappear. When the temperature is sufficiently high the linear dependence of γ on I, typical of a rigid rotor, is observed.

In fig. 7 the moment of inertia is displayed versus the angular momentum for various temperatures. The lowest isotherms show the dramatic decrease of moment of inertia due to pairing. The antipairing effect of the angular momentum is visible in the rapidly rising moment of inertia as the angular momentum increases. The cusps appearing in the lowest isotherms are associated with the disappearance of pairing. In the vicinity of these cusps the moment of inertia assumes values much above the average. This is due to the presence of high spin levels ($h_{9/2}$ for protons and $g_{9/2}$ for neutrons) close to the Fermi surface. The relevance of these levels decreases as the angular momentum increases because the quasiparticles occupy a larger number of levels thus producing an average over many spins. The higher isotherms show a rapid flattening of the fluctuations with the consequent achievement of a constant moment of inertia at all angular momenta. In fig. 8 the moment of inertia is plotted versus the square of the angular velocity for various temperatures. The main feature of this diagram is the absence of the backbending. The angular velocity, for the lowest isotherms, remains almost constant without backbending, while the moment of inertia rapidly increases. The constancy of angular velocity with angular momentum at low temperatures suggests that the dynamical behavior of the system is closer to that of an oscillator than to that of a rotor.

Figure 7 is very interesting insofar as it gives a direct answer concerning the validity of the spin cut-off approximation in level density calculations (see eq. (14) and eq. (15)). Among other things, such an approximation implies that the spin cut-off parameter depends only upon the temperature and not upon the angular momentum. Recalling that $\sigma^2 = \hbar^{-2}\mathcal{J}T$ one can see that, along a given isotherm, the angular momentum dependence of σ^2 is the same as that of $\mathcal{J}$. So, fig. 7 shows that at low temperatures the

spin cut-off approximation is rather poor because of the change in the moment of inertia due both to pairing and to shell effects associated with the various values of the angular momentum. At higher temperatures both pairing and shell effects disappear, the moment of inertia becomes independent of angular momentum, and the spin cut-off parameter becomes a rather good approximation.

7. Conclusion

Perhaps the most remarkable conclusion to be drawn from the present analysis is the great simplicity which is achieved by considering the pairing-angular momentum interaction in terms of the average rotational properties of nuclei. The study of individual quantum mechanical levels or bands requires a very detailed knowledge of the nuclear Hamiltonian and very intricate numerical calculations are necessary in order to exploit such a knowledge. By considering averages over many levels in an inherently simpler spherical nucleus, one may hope that the detailed non-essential features of the residual interactions may be "integrated out", thus leaving a clearer picture of the essential traits of the nuclear behavior. This we have tried to do theoretically, this still needs to be done experimentally.

It is quite possible that a much better understanding of the interrelation between pairing, angular momentum and excitation energy may be obtained from the study of the average properties of spherical nuclei than from the detailed analysis of the rotational or vibrational bands in deformed nuclei.

Footnotes and References

1) For a review of the theories on level densities see: a) T. Ericson, Advan. Phys. 9 (1960) 425; b) J. R. Huizenga and L. G. Moretto, Ann. Rev. Nucl. Phys. 22 (1972) 427

2) C. Bloch, Phys. Rev. 93 (1954) 1094

3) R. A. Sorensen, Rev. Mod. Phys. 45 (1973) 353 and references therein

4) A. Johnson, H. Ryde, and J. Starkier, Phys. Letters 34B (1971) 605

5) A. Johnson, H. Ryde, and S. A. Hjorth, Nucl. Phys. A179 (1972) 753

6) H. Buescher, W. F. Davidson, R. M. Lieder, and C. Mayer-Böricke, Phys. Letters 40B (1972) 449

7) R. M. Lieder, H. Beuscher, W. F. Davidson, P. Jahn, H. J. Probst, and C. Mayer-Böricke, Phys. Letters 39B (1972) 196

8) P. Thieberger, A. W. Sunyar, P. C. Rogers, N. Lark, O. C. Kistner, E. der Mateosian, S. C. Cochavi, and E. A. Auerbach, Phys. Rev. Letters 28 (1972) 972

9) T. Kammuri, Prog. Theor. Phys. 31 (1964) 595

10) L. G. Moretto, Phys. Letters 35B (1971) 374

11) L. G. Moretto, Nucl. Phys. A185 (1972) 145

12) L. G. Moretto, Nucl. Phys. A216 (1973) 1

13) P. Decowski, W. Grochulski, A. Marcinkowski, K. Siwek, and Z. Wilhelmi, Nucl. Phys. A110 (1968) 129

14) L. G. Moretto, Phys. Letters 44B (1973) 494

15) M. Sano and S. Yamasaki, Prog. Theor. Phys. 29 (1963) 317

16) L. G. Moretto, Phys. Letters 40B (1972) 1

17) L. G. Moretto, Phys. Letters 46B (1973) 20

Figure Captions

Fig. 1. Angular velocity as a function of angular momentum for various temperatures. The solid line rising from left to right corresponds to a rigid rotor. The solid line descending from left to right corresponds to the limit of $T = 0$. In fig. 1a the calculation has been performed by using the most probable values of Δ; the temperature is $0.1\ T_{cr}$ for the uppermost thin line and it increases in steps of $0.1\ T_{cr}$ for the lower lines. In fig. 1b the calculation has been performed by using the average values of Δ. Notice that the bottom thin line corresponds to $T = T_{cr}$.

Fig. 2. Moment of inertia as a function of angular momentum. In fig. 2a the calculation has been performed by using the most probable values of Δ. The temperature sequence for the thin lines from bottom to top is 0, 0.2, 0.4, 0.6, $0.8\ T_{cr}$. In fig. 2b the calculation has been performed by using the average values of Δ. The temperature sequence is 0, 0.2, 0.4, 0.6, 0.8, $1.0\ T_{cr}$.

Fig. 3. Moment of inertia as a function of the square of the angular velocity. In fig. 3a the most probable values of Δ have been used. The temperatures range from 0 to $0.9\ T_{cr}$ in steps of $0.1\ T_{cr}$. In fig. 3b the average values of Δ have been used. The temperatures range from 0.1 and $1.0\ T_{cr}$ in steps of $0.1\ T_{cr}$. The dotted lines in both figures correspond to constant angular momentum. The leftmost dotted line corresponds to $I = 0.2\ I_{cr}$. The remaining dotted lines are plotted in steps of $0.2\ I_{cr}$.

Fig. 4. Angular velocity as a function of angular momentum for a rectangular distribution of spin projections (thick lines). The thin lines correspond to a δ distribution in spin projections.

Fig. 5. Various shapes of the yrast line for various models. The dashed line corresponds to a rigid moment of inertia. The thin line corresponds to a δ distribution in spin projections. The thick line corresponds to a rectangular distribution in spin projection.

Fig. 6. Angular velocity as a function of angular momentum for the proton a) and neutron b) components of ^{220}Rn for various temperatures. The lowest temperature value and the temperature spacing between the various isotherms is given on the top caption.

Fig. 7. Moment of inertia as a function of angular momentum for the proton a) and neutron b) components of ^{220}Rn for various temperatures. The lowest temperature value and the temperature spacing between the various isotherms is given on the top caption.

Fig. 8. Moment of inertia as a function of the square of angular velocity for the proton a) and neutron b) components of ^{220}Rn for various temperatures. The lowest temperature value and the temperature spacing between the various isotherms is given on the top caption.

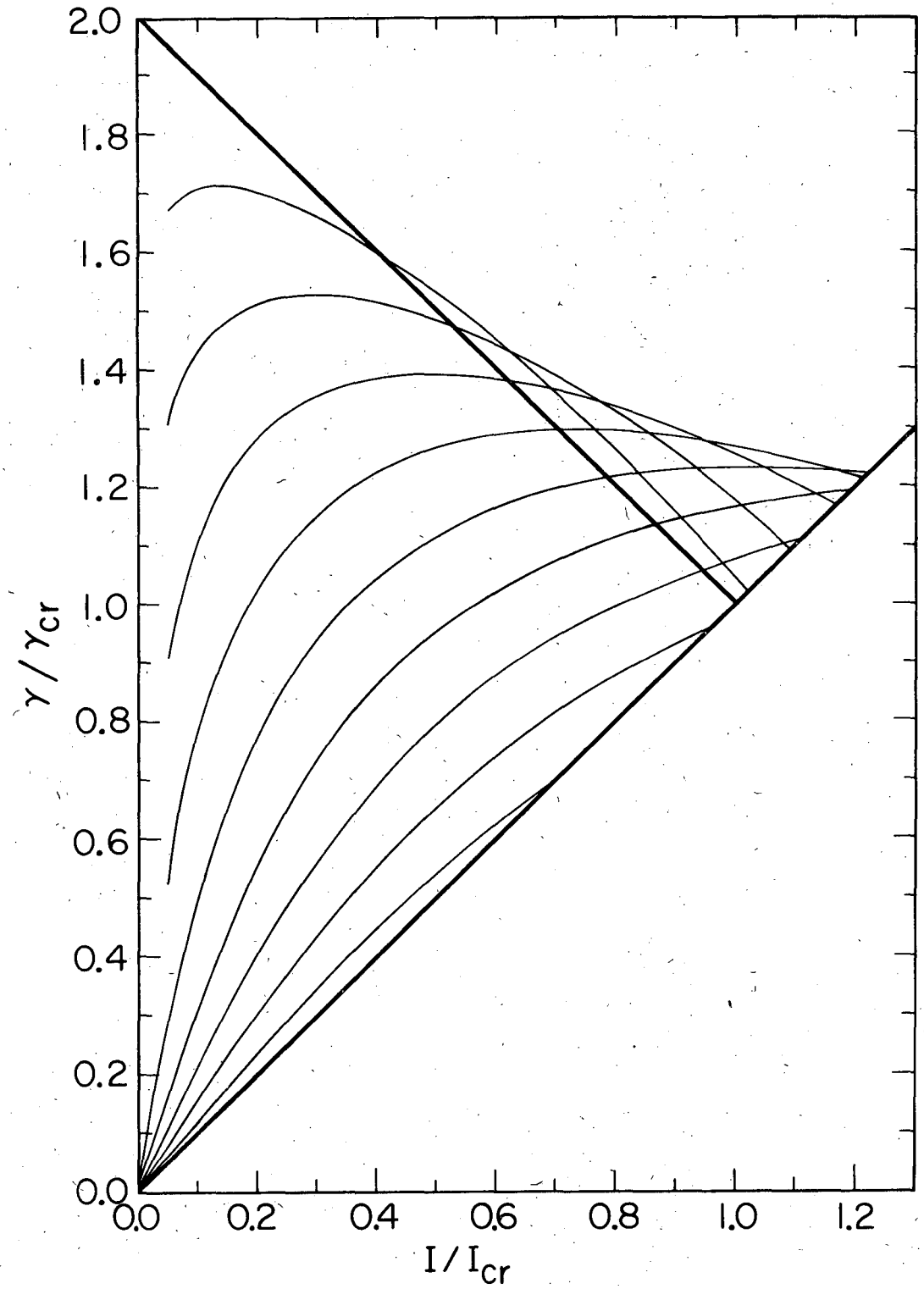

XBL7311-4584

Fig. 1a

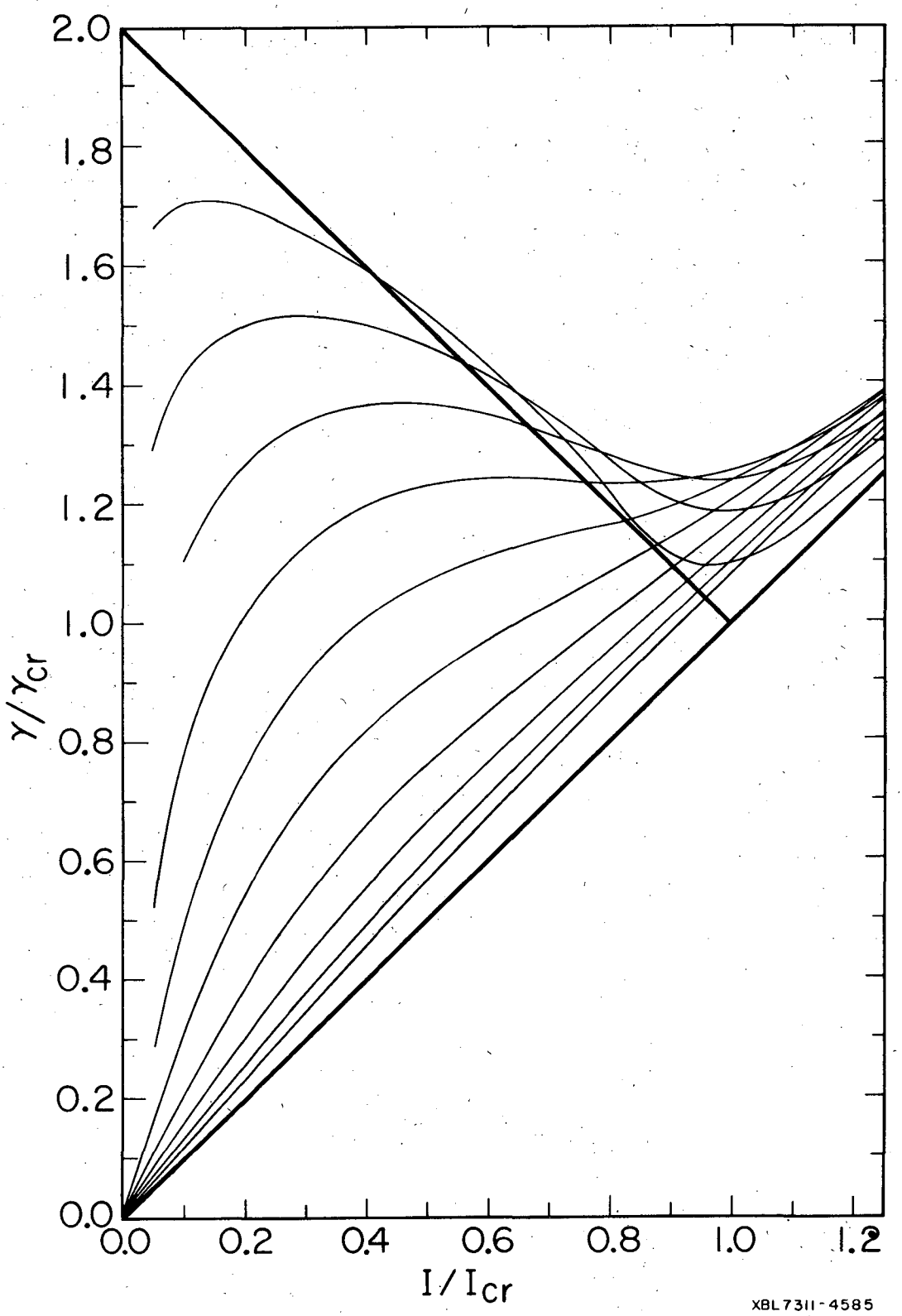
2.0
1.8
1.6
1.4
1.2
1.0
0.8
0.6
0.4
0.2
0.0
γ/γcr
0.0
0.2
0.4
0.6
0.8
1.0
1.2
I/Icr
XBL7311-4585

Fig. 1b

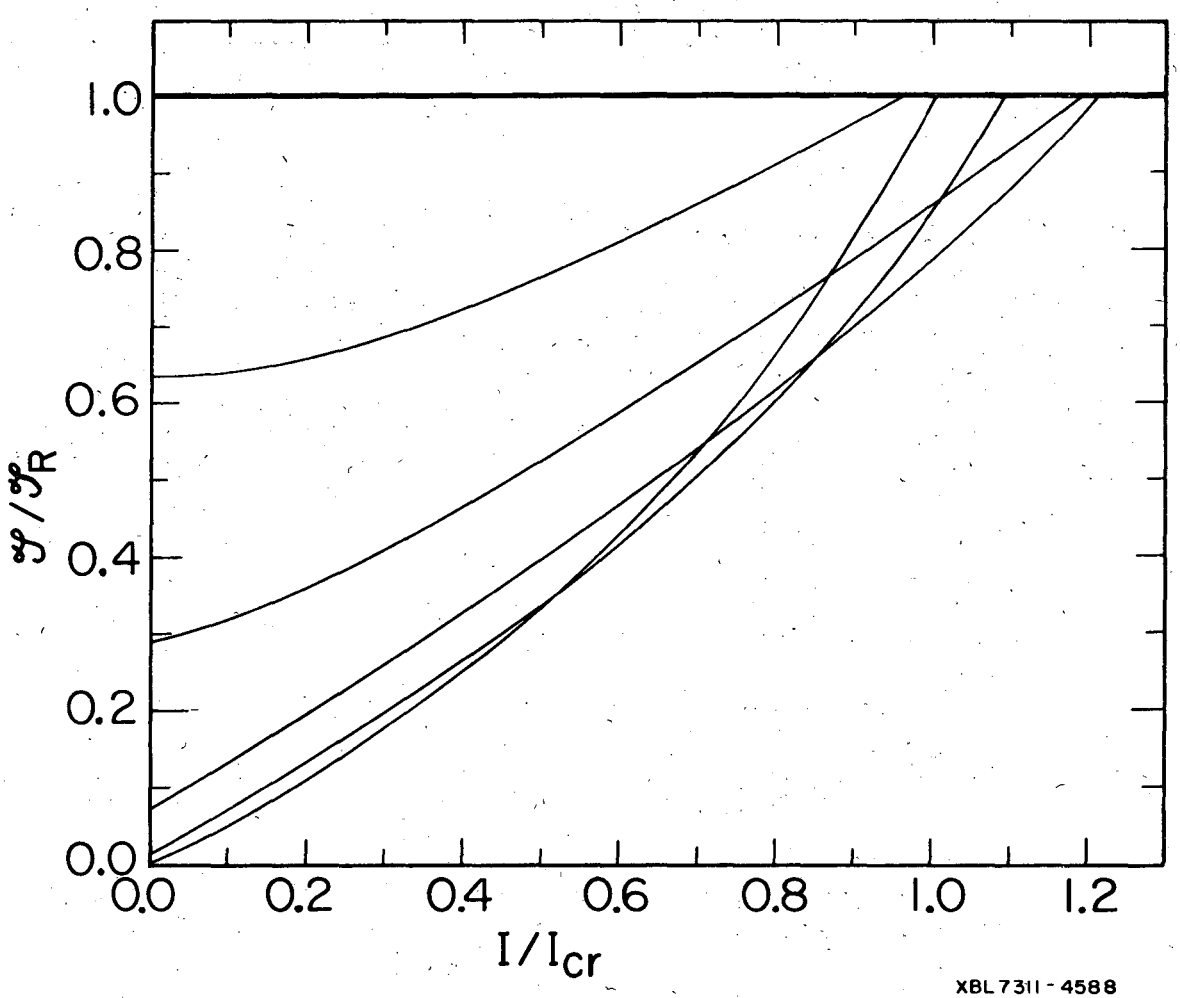
1.0
0.8
0.6
0.4
0.2
0.0
$\mathcal{J}/\mathcal{J}_R$
0.0
0.2
0.4
0.6
0.8
1.0
1.2
I/I_{cr}
XBL 7311-4588

Fig. 2a

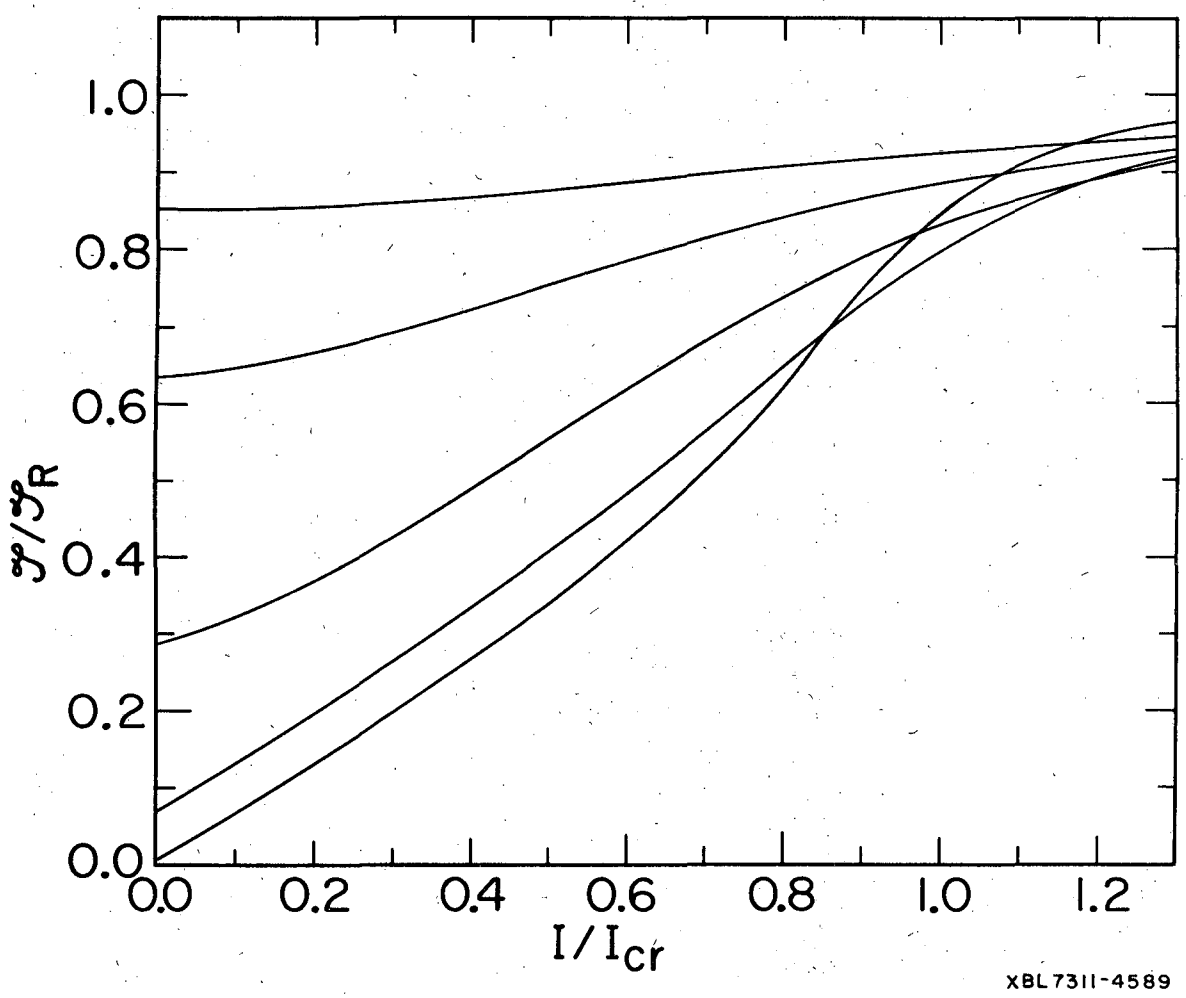
1.0
0.8
0.6
0.4
0.2
0.0
$\mathcal{J}/\mathcal{J}_R$
0.0
0.2
0.4
0.6
0.8
1.0
1.2
I/I_{cr}
XBL7311-4589

Fig. 2b

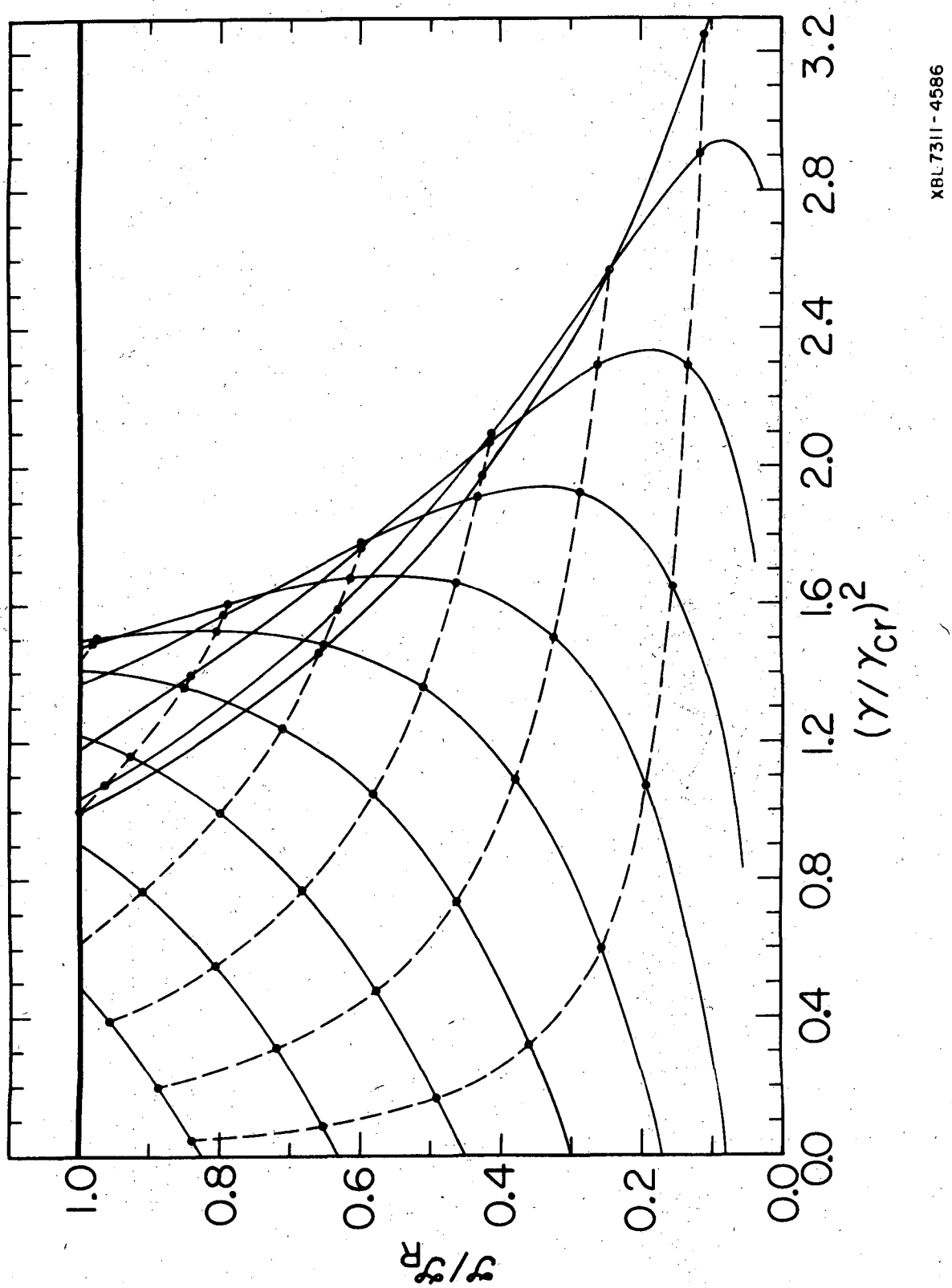
1.0
0.8
0.6
0.4
0.2
0.0
$\mathcal{T}/\mathcal{T}_R$
0.0
0.4
0.8
1.2
1.6
2.0
2.4
2.8
3.2
$(\gamma/\gamma_{cr})^2$
XBL 7311-4586

Fig. 3a

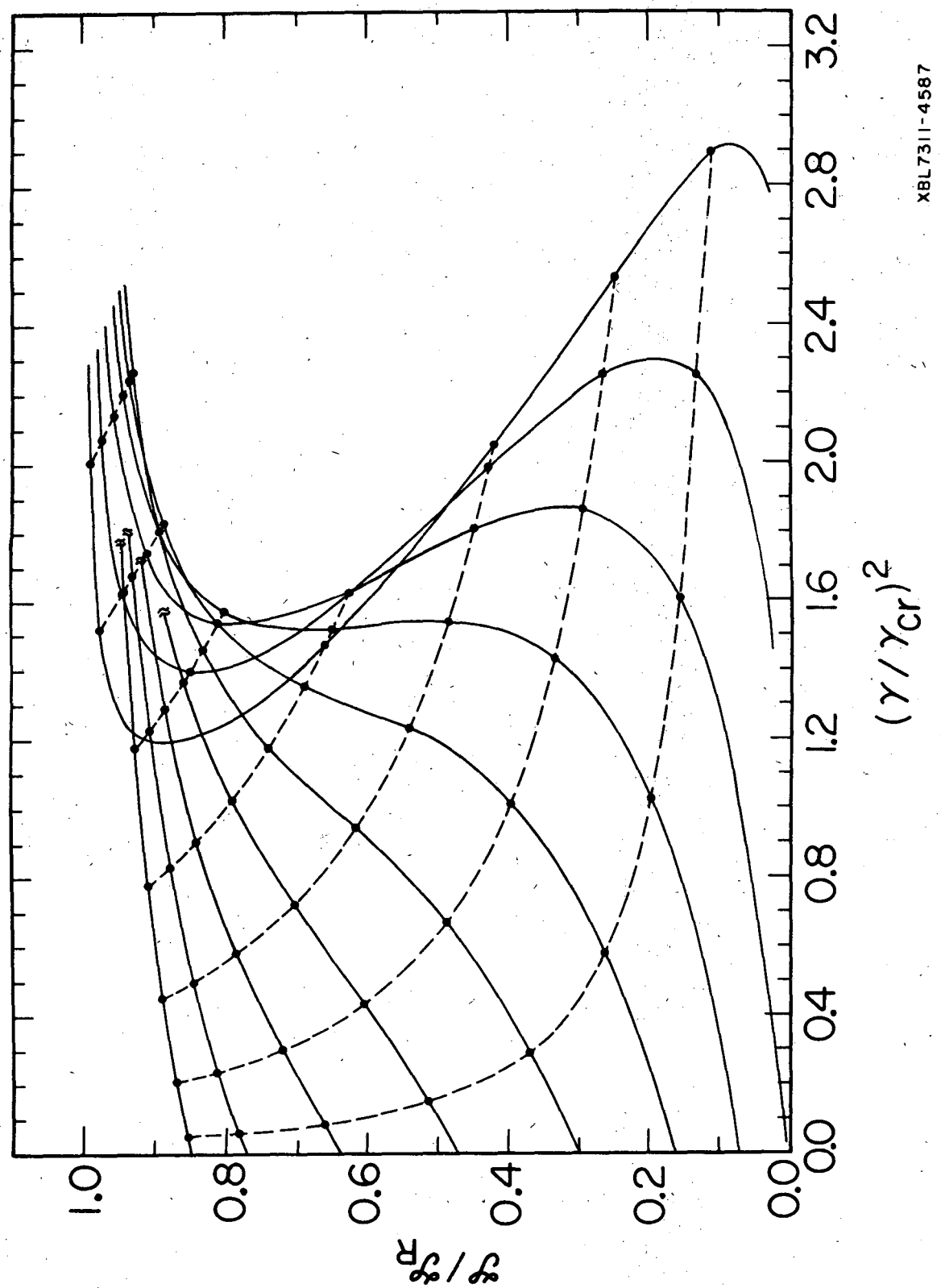
XBL7311-4587
$(\gamma/\gamma_{cr})^2$
0.0
0.4
0.8
1.2
1.6
2.0
2.4
2.8
3.2
$\mathcal{J}/\mathcal{J}_R$
0.0
0.2
0.4
0.6
0.8
1.0

Fig. 3b

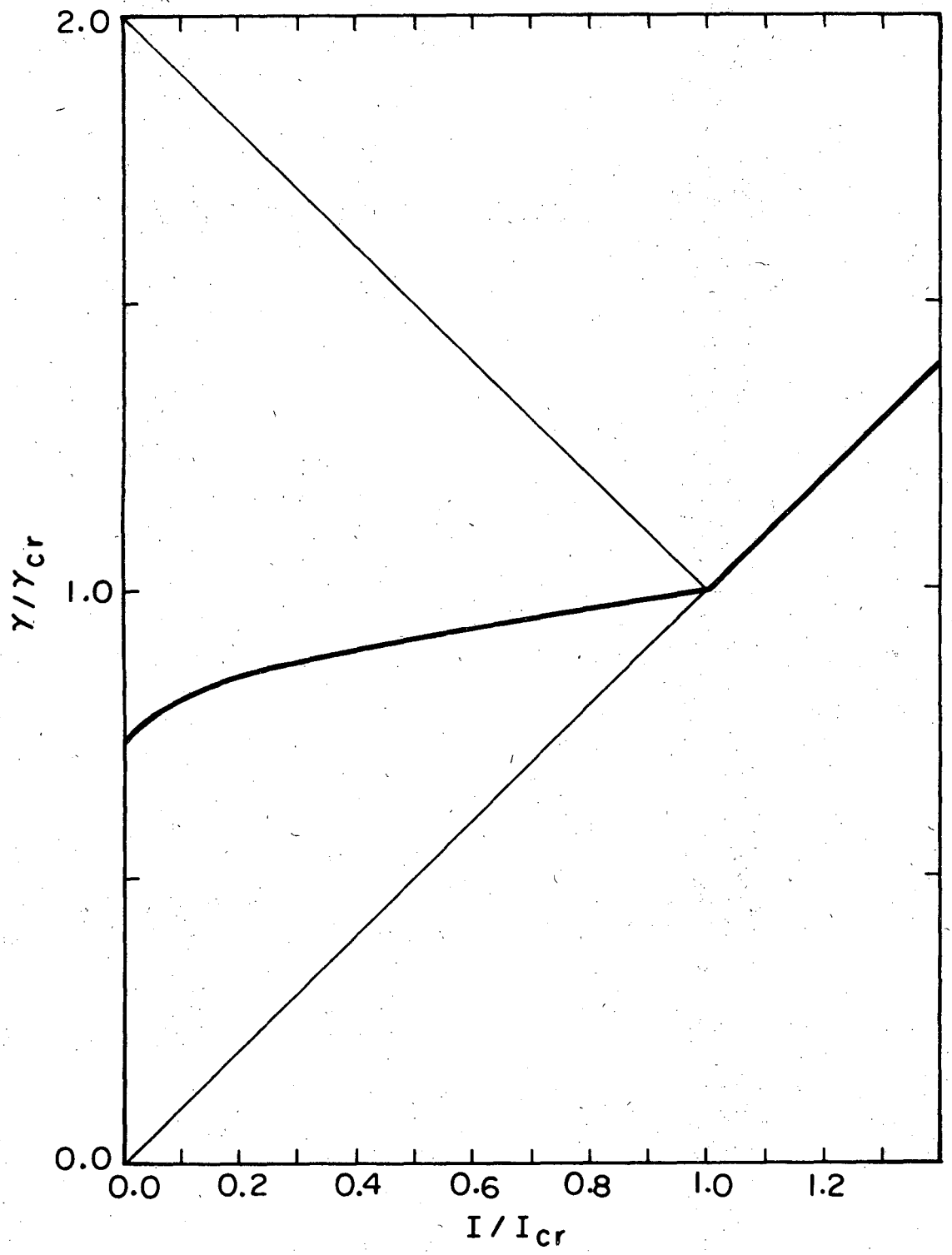

XBL735-2831

Fig. 4

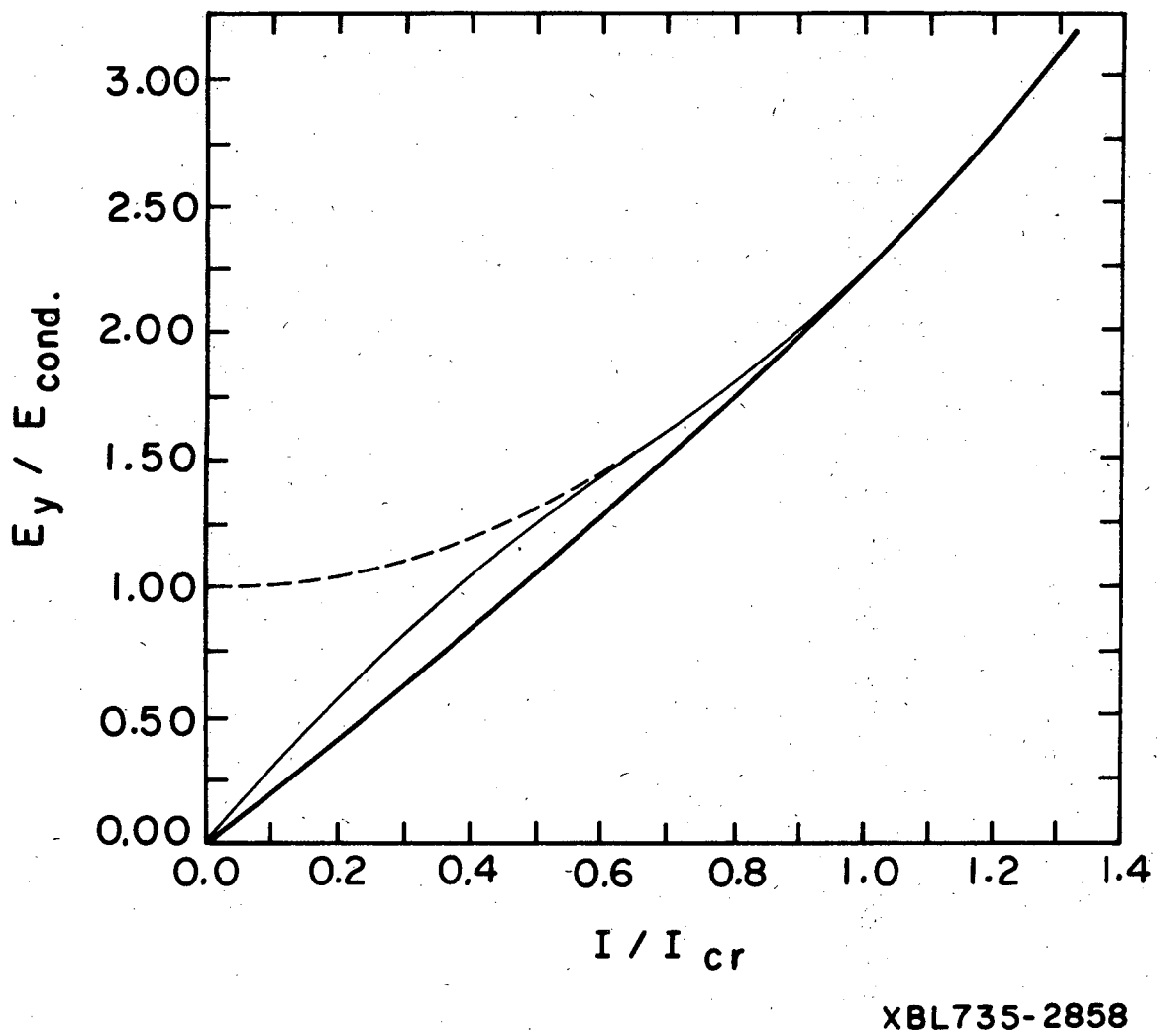
3.00
2.50
2.00
1.50
1.00
0.50
0.00
E_y / $E_{cond.}$
0.0
0.2
0.4
0.6
0.8
1.0
1.2
1.4
I / I_{cr}
XBL735-2858

Fig. 5

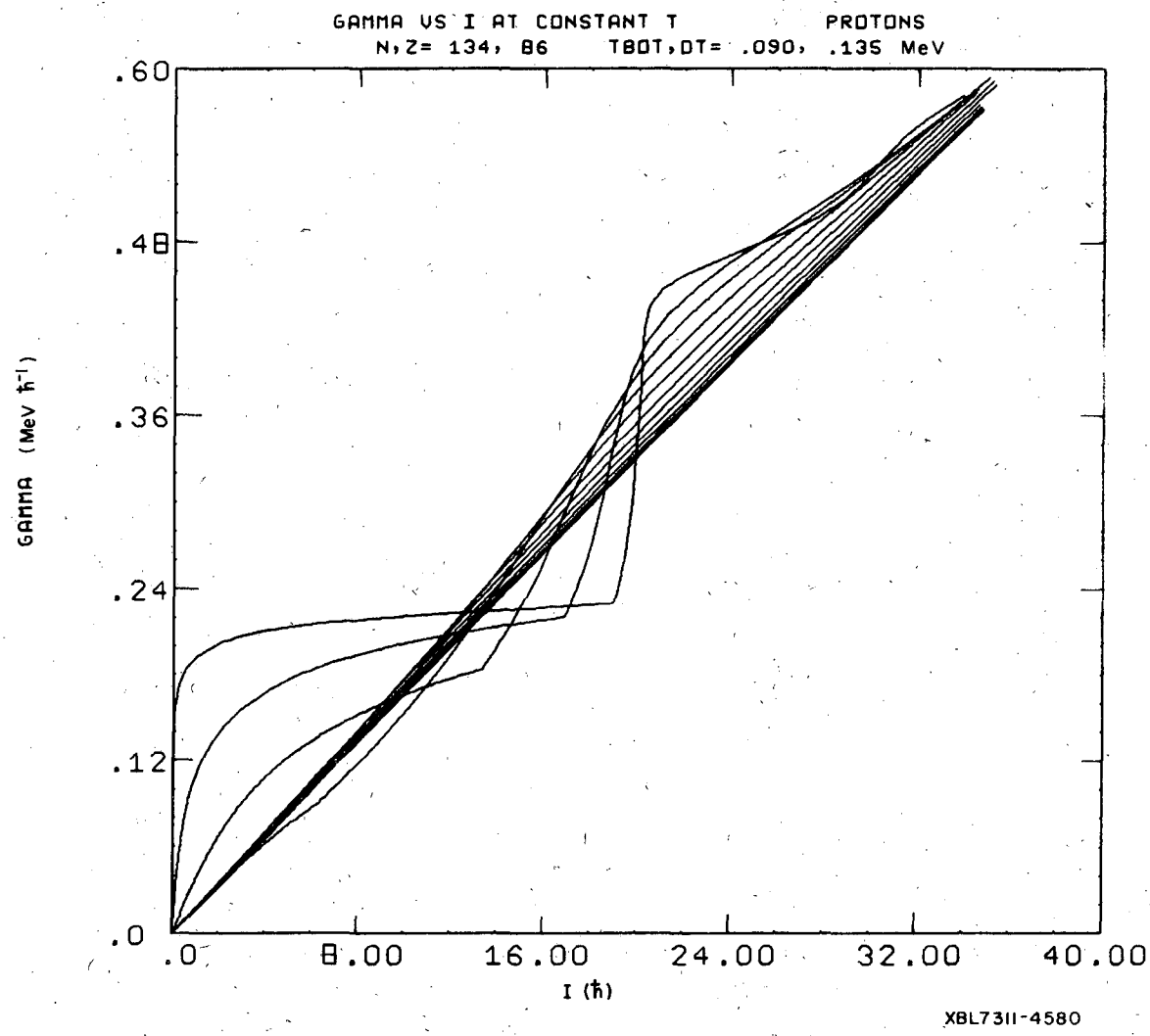
GAMMA VS I AT CONSTANT T
PROTONS
N,Z= 134, 86
TBOT,DT= .090, .135 MeV
GAMMA (MeV ħ⁻¹)
.60
.48
.36
.24
.12
.0
.0
8.00
16.00
24.00
32.00
40.00
I (ħ)
XBL7311-4580

Fig. 6a

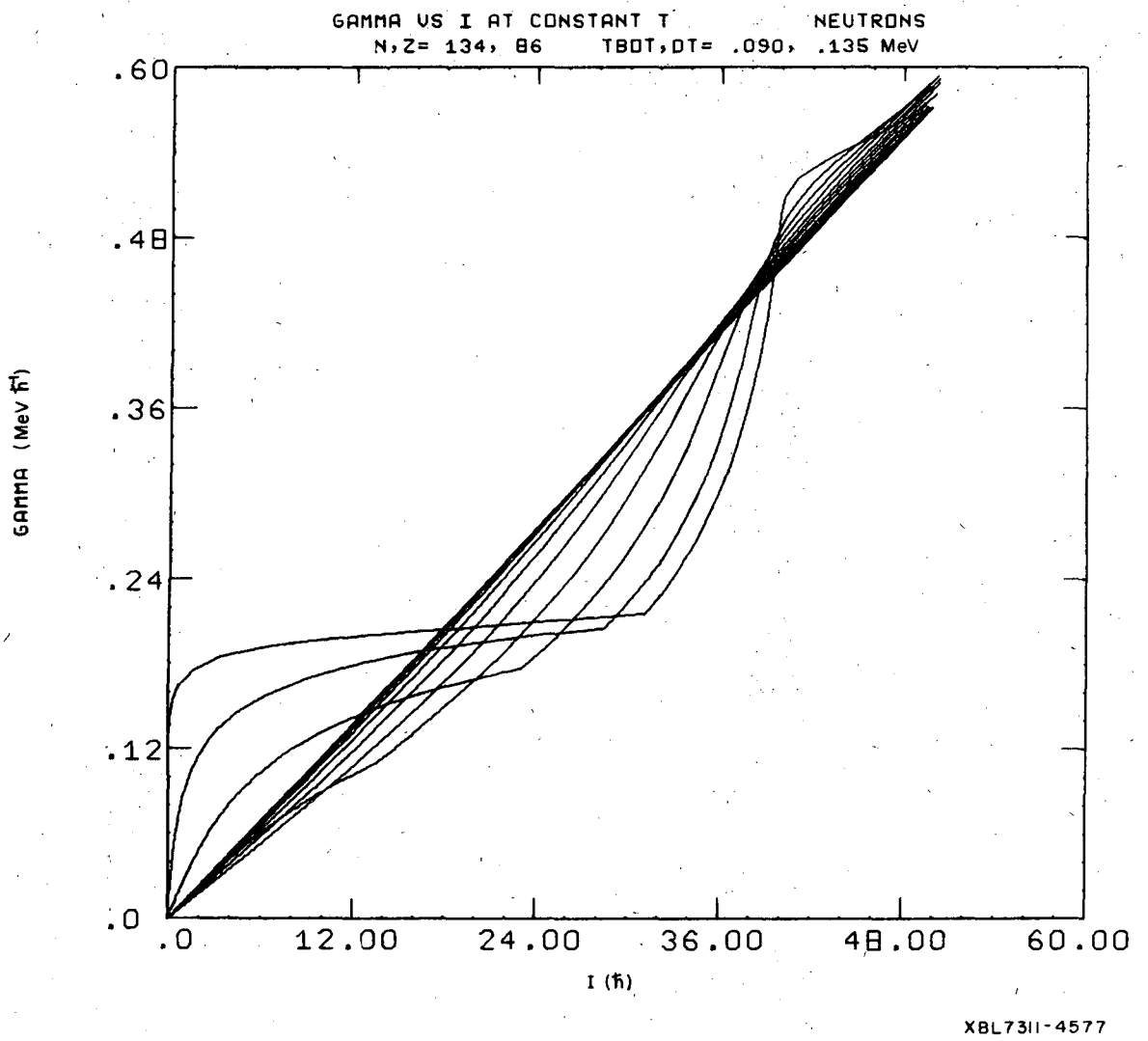
GAMMA VS I AT CONSTANT T
NEUTRONS
N,Z= 134, 86
TBOT,DT= .090, .135 MeV
.60
.48
.36
.24
.12
.0
GAMMA (MeV ħ⁻¹)
.0
12.00
24.00
36.00
48.00
60.00
I (ħ)
XBL7311-4577

Fig. 6b

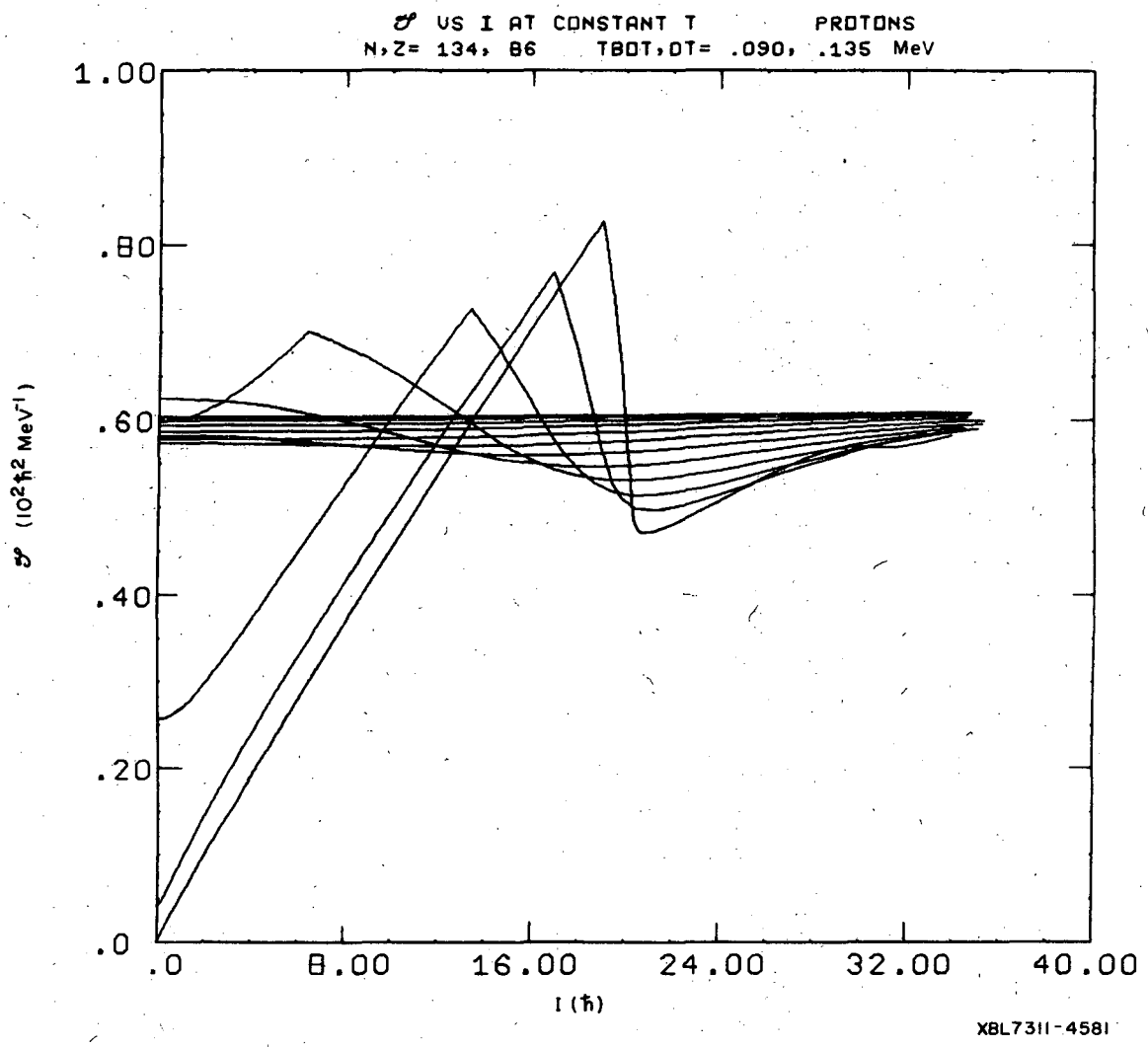
𝒥 VS I AT CONSTANT T PROTONS
N,Z= 134, 86 TBOT,DT= .090, .135 MeV
1.00
.80
.60
.40
.20
.0
𝒥 (10²ħ² MeV⁻¹)
.0
8.00
16.00
24.00
32.00
40.00
I (ħ)
XBL7311-4581

Fig. 7a

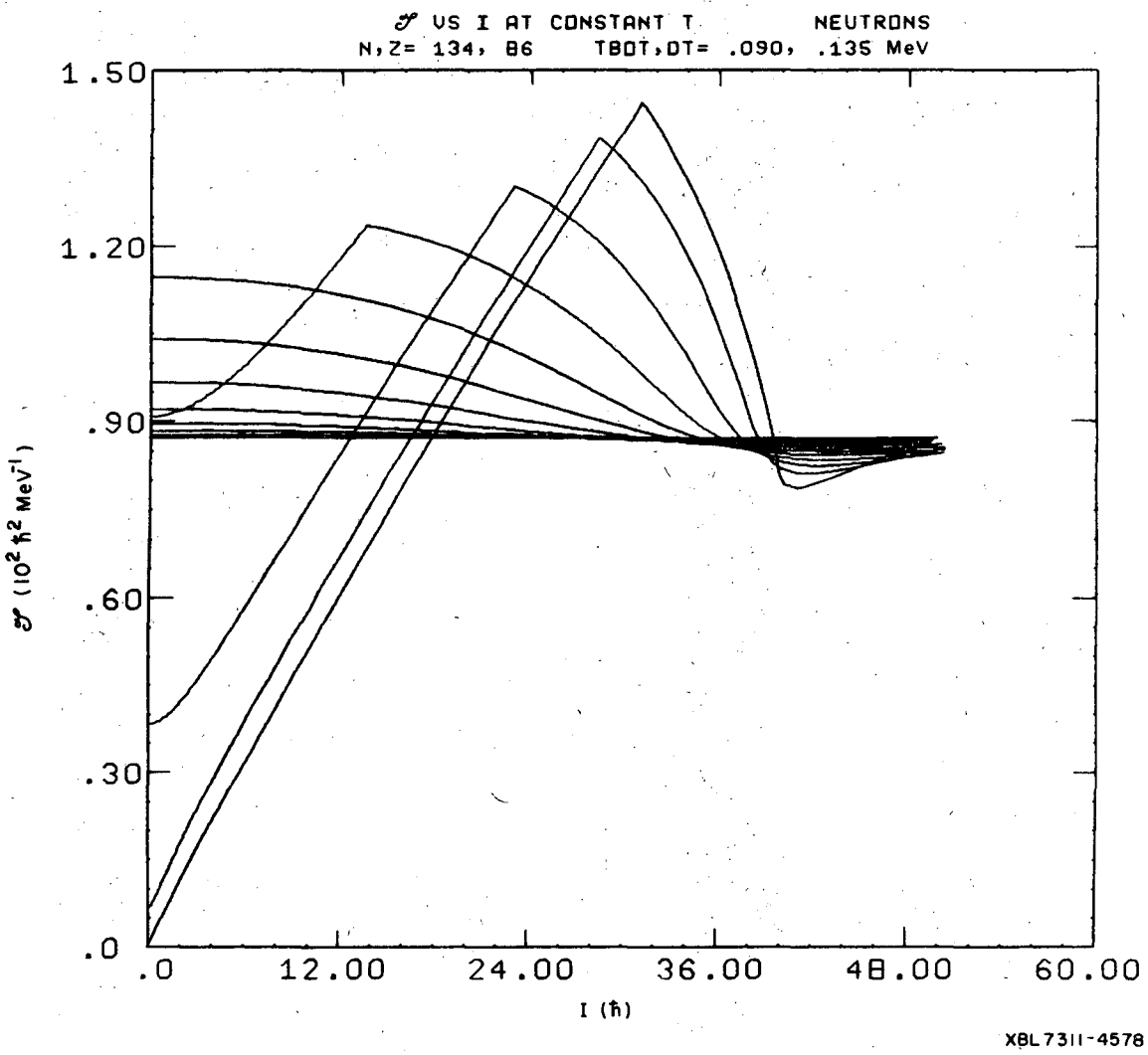
𝒥 VS I AT CONSTANT T NEUTRONS
N,Z= 134, 86 TBOT,DT= .090, .135 MeV
1.50
1.20
.90
.60
.30
.0
𝒥 (10² ħ² MeV⁻¹)
.0
12.00
24.00
36.00
48.00
60.00
I (ħ)
XBL7311-4578

Fig. 7b

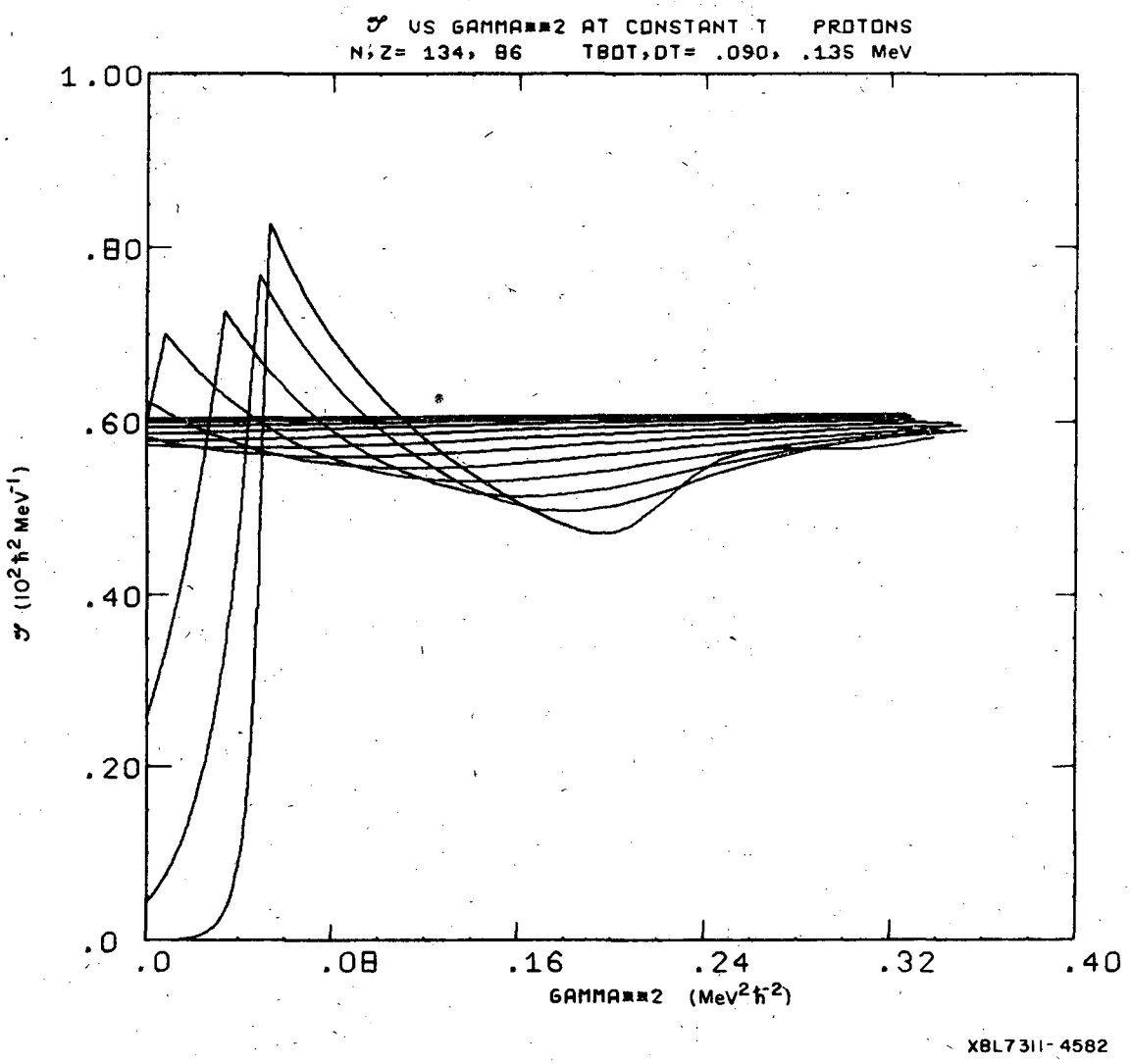
𝒟 VS GAMMA**2 AT CONSTANT T PROTONS
N,Z= 134, 86 TBOT,DT= .090, .135 MeV
1.00
.80
.60
.40
.20
.0
.0
.08
.16
.24
.32
.40
𝒟 (10²ħ² MeV⁻¹)
GAMMA**2 (MeV²ħ⁻²)
XBL7311-4582

Fig. 8a

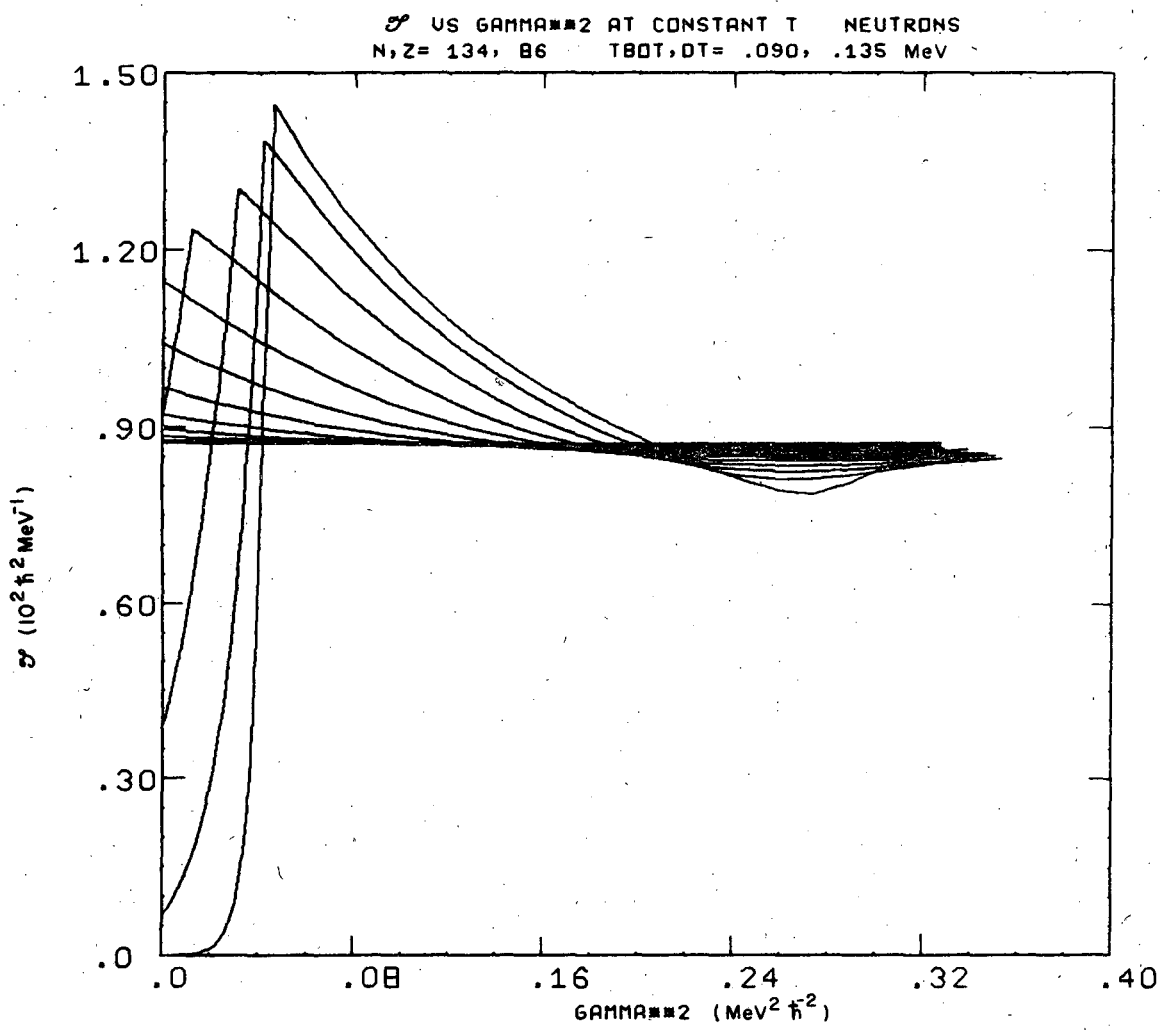

XBL7311-4579

Fig. 8b

LEGAL NOTICE

This report was prepared as an account of work sponsored by the United States Government. Neither the United States nor the United States Atomic Energy Commission, nor any of their employees, nor any of their contractors, subcontractors, or their employees, makes any warranty, express or implied, or assumes any legal liability or responsibility for the accuracy, completeness or usefulness of any information, apparatus, product or process disclosed, or represents that its use would not infringe privately owned rights.

TECHNICAL INFORMATION DIVISION
LAWRENCE BERKELEY LABORATORY
UNIVERSITY OF CALIFORNIA
BERKELEY, CALIFORNIA 94720